THz–generation in semiconductor superlattice in the external tilted magnetic field

Vladimir V. Makarov[a,b], Vladimir A. Maksimenko[a,b], Anton O. Selskii[a], Alexey N. Pavlov[a,c], Marina V. Khramova[d], Alexey A. Koronovskii[b,a], Alexander E. Hramov[a,b]

[a]Research and Educational Center "Nonlinear Dynamics of Complex Systems", Saratov State Technical University, Polytechnicheskaya Str. 77, Saratov, 410054, Russia;
[b]Faculty of Nonlinear Processes, Saratov State University, Astrakhanskaya Str. 83, Saratov, 410012, Russia;
[c]Physics Dept., Saratov State University, Astrakhanskaya Str. 83, Saratov, 410012, Russia;
[d]Faculty of Computer Sciences and Information Technologies, Saratov State University, Astrakhanskaya Str. 83, Saratov, 410012, Russia

ABSTRACT

We study effects of the external tilted magnetic field on the generation of sub-THz/THz oscillations in the semiconductor superlattice. We show that this field provides the increased power of harmonics in the THz range. Changing the tilt angle essentially influences the distribution of spectral power of current oscillations in the semiconductor superlattice.

Keywords: semiconductor, superlattice, THz-generation, magnetic field, space charge, current oscillations

1. INTRODUCTION

The development of semiconductor devices working in sub-THz and THz ranges is of a high importance for a wide range of applications[1] including astrophysics, medicine, etc.[2,3] In particular, one of the most challenging tasks of modern electronics is the elaboration of technically available sub-millimeter wavelength devices operating at room temperature.[4] Typically, the use of nano- and microstructure-based setups such as quantum-cascade lasers (QCLs), transferred electron devices (TEDs) and other devices that exhibit negative differential conductance is a widely used approach in the related studies.[5,6] Nevertheless, characteristics of such devices are strongly limited by their physical dimensions such as the minimal length of active media in TEDs that strongly influences the frequency of oscillations. In order to improve properties of such devices, external influences such as, e.g., electric and/or magnetic fields can be applied.[7]

The semiconductor superlattice is related to the promising devices demonstrating the negative differential conductance and working in sub-THz/THz range. Semiconductor superlattices are composed from alternating layers of different semiconductor materials (two or more) with different bandwidth. Such periodic structure promotes the formation of minibands in which electrons can travel along the semiconductor superlattice. If the product of the carrier concentration within the device and the sample length exceeds a critical value, the NDC triggers the formation of propagating charge domains, which could be utilized both for generation and amplification of sub-THz/THz radiation.[8,9]

Recently, we have shown that the drift velocity of electrons in the semiconductor superlattice can be effectively controlled by an external tilted magnetic field.[10,11] In this paper we study how the external tilted magnetic field can be utilized to increase the power of the highest harmonics of the semiconductor superlattice in THz range.

Further author information: (Send correspondence to A.E. Hramov)
A.E. Hramov: E-mail: hramovae@gmail.com, Telephone: +7 8452 51 42 94

Dynamics and Fluctuations in Biomedical Photonics XII, edited by Valery V. Tuchin, Kirill V. Larin, Martin J. Leahy, Ruikang K. Wang, Proc. of SPIE Vol. 9322, 932211 · © 2015 SPIE
CCC code: 1605-7422/15/$18 · doi: 10.1117/12.2076737

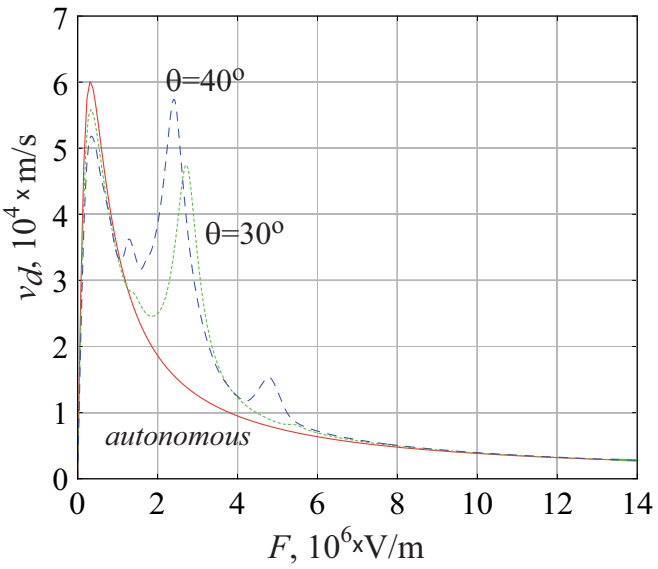

Figure 1. Drift velocity of electron in the superlattice for $B = 0$ (solid curve, red online), $B = 12$ and $\theta = 30^\circ$ (dotted curve, green online), $B = 12$ and $\theta = 40^\circ$ (dashed curve, blue online).

2. DRIFT VELOCITY

Within a semiclassical assumption, the drift velocity v_d of a single electron under the influence of electric field $\mathbf{F} = (-F, 0, 0)$ and magnetic field $\mathbf{B} = (B\cos\theta, 0, B\sin\theta)$ can be written as[12,13]

$$v_d = \frac{1}{\tau}\int_0^\infty v_x(t)e^{-t/\tau}\,dt, \tag{1}$$

where τ is the scattering time of electron, $v_x(t)$ is the x-component of velocity, determined by the motion equation of electron in the semiconductor superlattice[14]

$$\ddot{p}_z + \hat{\omega}_c^2 p_z = C\sin(Kp_z - \omega_B t - \phi), \tag{2}$$

where

$$C = -\frac{\Delta d m^* \hat{\omega}_c^2 \tan\theta}{2\hbar}, \tag{3}$$

$$K = \frac{d\tan\theta}{\hbar}, \tag{4}$$

$$\phi = \frac{d}{\hbar}\left(p_z(0)\tan\theta + p_x(0)\right). \tag{5}$$

In the equations (2) – (5), $\mathbf{p} = (p_x, p_y, p_z)$ is the electron's impulse, Δ is the superlattice miniband width, d is the layer width, $m^* = 0.067m_e$ is the effective mass of electron in GaAs, m_e is the free electron mass, $\omega_B = eFd/\hbar$ is the cyclic Bloch frequency, $\hat{\omega}_c = \omega_c\cos\theta$ is the cyclic cyclotron frequency along the drift axis Ox, and $\omega_c = eB/m^*$. The equation (2) that can be solved only numerically, determines other components of the impulse

$$p_x = eFt - p_z\tan\theta, \qquad p_y = \frac{\dot{p}_z}{\bar{\omega}_c}, \tag{6}$$

and the velocity of electron

$$\dot{x} = \frac{d\Delta}{2\hbar}\sin(Kp_z - \omega_B t - \phi), \qquad \dot{y} = \frac{\dot{p}_z}{\bar{\omega}_c m^*}, \qquad \dot{z} = \frac{p_z}{m^*}. \tag{7}$$

The latter, in turn, allows us to determine the drift velocity of electron (1) that also depends from the electron's impulse $\mathbf{p}_0 = (p_{x0}, p_{y0}, p_{z0})$

$$v_d = v_d(\mathbf{p}_0). \tag{8}$$

Drift velocity v_d can be determined analytically when the magnetic field is absent $B = 0$.[12] For initial conditions $p_{0x} = 0$, $p_{0y} = 0$, $p_{0z} = 0$, it has the following form

$$v_d = \frac{d\Delta}{2\hbar} \frac{\tau\omega_B}{(1 + \tau^2\omega_B^2)}. \tag{9}$$

Dependencies of the drift velocity from electric field for the semiconductor superlattice without external magnetic field and for the semiconductor superlattice with an applied magnetic field for two different tilt angles are shown in Fig. 1. According to this Figure, applying the external field implies significant changes in the dynamics of electron in the active media. In contrast to the case of $B = 0$ (solid line, red online) curves corresponding to the applied magnetic field exhibit multiple maxima. The first maximum, for the lowest value of F, also exists when $B = 0$ and is associated with the onset of Bloch oscillations. All other maxima occur because of the enhanced acceleration of electrons on the Bloch-cyclotron resonances. For the case of $\theta = 40°$, the drift velocity is sufficiently higher, and the maxima corresponding to the Bloch-cyclotron resonances are more pronounced in comparison with $\theta = 30°$. This circumstance allows us to control the system dynamics by changing the tilt angle of the applied magnetic field.

3. COLLECTIVE ELECTRON DYNAMICS

To describe a collective electron transport in the superlattice we use an earlier described model,[11,15] with parameters of the semiconductor superlattice taken from recent experiments.[16] The miniband transport region is discretized into $N = 480$ layers, each of width $\delta x = 0.24\,\text{nm}$, that is small enough to ensure convergence of the numerical scheme. The discretized current continuity equation is

$$e\delta x \frac{dn_m}{dt} = J_{m-1} - J_m, \qquad m = 1 \ldots N, \tag{10}$$

where $e > 0$ is the electron charge, n_m is the charge density at the right-hand edge of m^{th} layer, at position $x = m\delta x$, and J_{m-1} and J_m are the current densities at the left and right hand boundaries of the m^{th} layer

$$J_m = en_m v_d\left(\overline{F}_m\right), \tag{11}$$

where $\overline{F}_m$ is the mean field in the m^{th} layer.[15] The drift velocity, $v_d(\overline{F})$, corresponding to electric field, $\overline{F}$, was described in Section 2.

The electric fields F_m and F_{m+1} at the left- and right-hand edges of the m^{th} layer respectively, are related to the discretized Poisson equation

$$F_{m+1} = \frac{e\delta x}{\varepsilon_0\varepsilon_r}(n_m - n_D) + F_m, \quad m = 1 \ldots N, \tag{12}$$

where ε_0 and $\varepsilon_r = 12.5$ are the absolute and the relative permittivities, respectively, and $n_D = 3 \times 10^{22}\ \text{m}^{-3}$ is the n-type doping density in the semiconductor superlattice layers. The current density injected into the contact layers of the semiconductor superlattice subjected to the field F_0 is $J_0 = \sigma F_0$, where $\sigma = 3788\ \text{Sm}^{-1}$ is the conductivity of the heavily-doped emitter.[15] The voltage, V_{sl}, dropped across the semiconductor superlattice defines a global constraint:

$$V_{sl} = U + \frac{\delta x}{2}\sum_{m=1}^{N}(F_m + F_{m+1}), \tag{13}$$

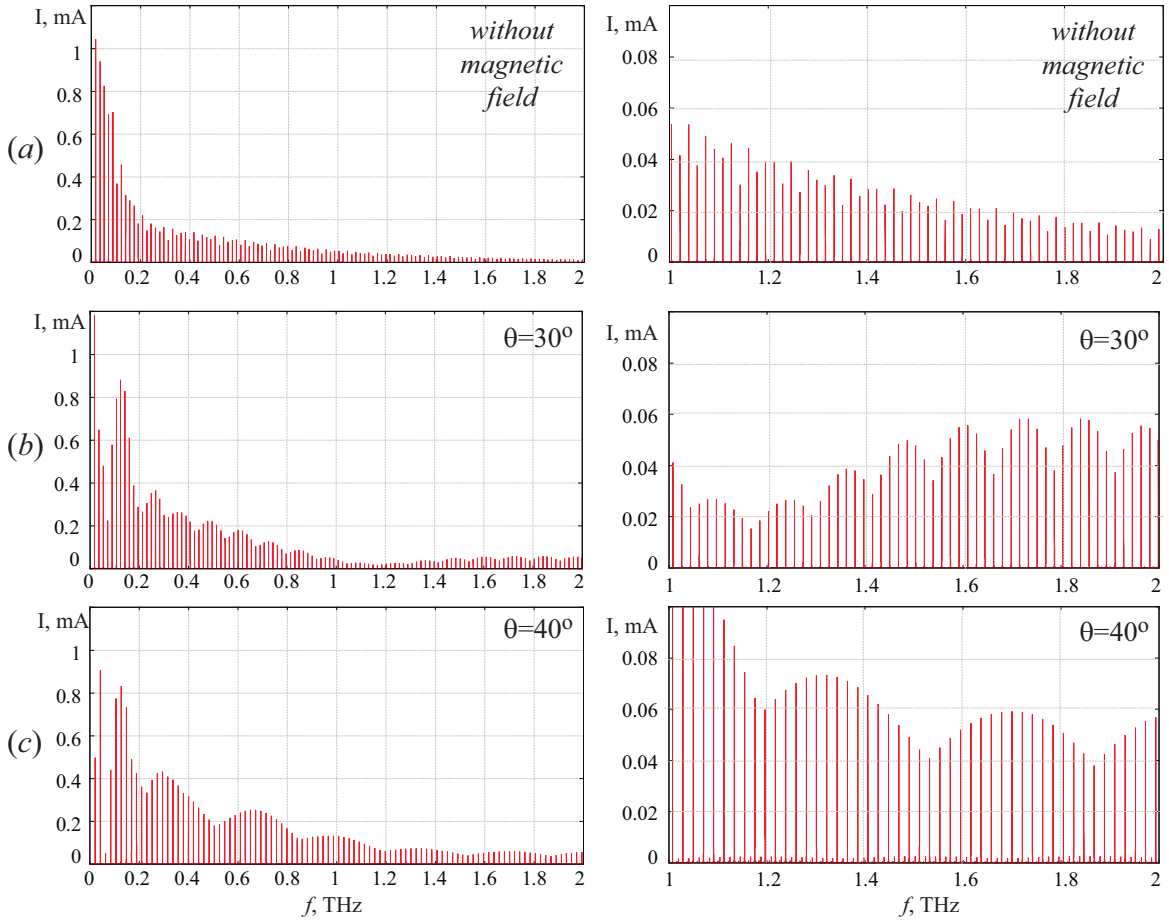

Figure 2. Amplitude spectra of current oscillations in the semiconductor superlattice: (a) $B = 0$, (b) $B = 12$ and $\theta = 30°$, (c) $B = 12$ and $\theta = 40°$. Frequency range 1–2 THz is shown in the right panel. Supply voltage applied to the semiconductor superlattice is $V_{sl} = 610$ mV.

where the voltage, U, dropped across the contacts includes the effect of charge accumulation and depletion in the emitter and collector regions, and the voltage across the contact resistance,[17] $R = 17\ \Omega$. The current through the device is

$$I(t) = \frac{A}{N+1} \sum_{m=0}^{N} J_m, \tag{14}$$

where $A = 5 \times 10^{-10}$ m^2 is the cross-sectional area of the semiconductor superlattice.[15,17]

To describe effects of the magnetic field on the dynamics of analyzed system, the Fourier spectra of current oscillations in the semiconductor superlattice were estimated (Fig. 2). For better representation, the range of 1–2 THz is illustrated in the right panel. When the magnetic field is absent (Fig. 2(a)), the amplitude of harmonics rapidly decreases till 200 GHz and then reduces almost linearly. In contrast, if magnetic field is applied at $\theta = 30°$ (see Fig. 2(b)), a sufficient reduction of spectral components near 70 GHz with the following maxima at 140 GHz appear. Besides, spectral amplitudes increase at frequencies above 1.1 THz, and they have significantly more power at 1–2 THz range as compared with Fig. 2(a). Increasing the tilt angle (see Fig. 2(c), $\theta = 40°$) results in the further swapping of the generation power to higher frequencies.

The obtained result can be illustrated using the spatial dynamics of charge traveling through the superlattice. The spatio-temporal distributions of electron concentration in the semiconductor superlattice are shown in Fig. 3. One can see, that the charge domains appear near the emitter of semiconductor superlattice when $B = 0$ (Fig. 3(a)). The charge concentration in the domain increases during its moving to the collector, whereupon

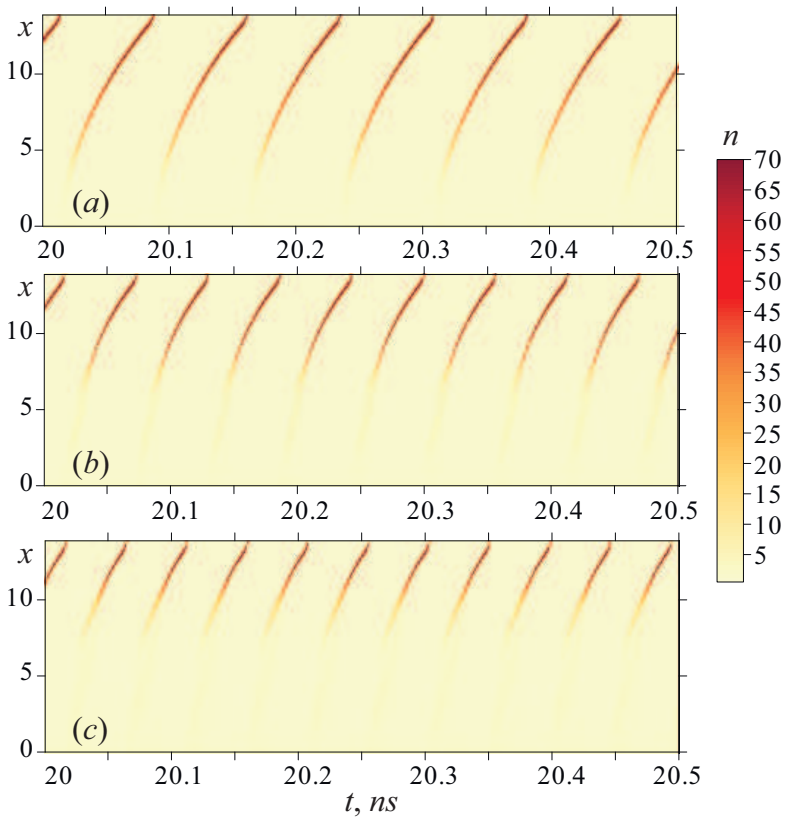

Figure 3. Spatio-temporal distributions of charge in the semiconductor superlattice: (a) $B = 0$, (b) $B = 12$ and $\theta = 30°$, (c) $B = 12°$ and $\theta = 40°$. The coordinate, x, and charge density, n, are given in non-dimensional units. Supply voltage applied to the semiconductor superlattice is $V_{sl} = 610$ mV.

the speed of the domain decreases. When the magnetic field is applied (Fig. 3(b)), the formation of the domain displaces to the middle of active media, that results in the increased speed, and, accordingly, the increased frequency of generation. This time domain reaches collector before it became too "heavy" and slow. The increasing of the tilt angle of the magnetic field (Fig. 3(c)) provides a further shifting of the domain emergence to the collector region, and the frequency increases. In fact, magnetic field enables us to artificially decrease the active media for moving domain and to increase the frequency of charge transport.

4. CONCLUSIONS

In this paper we studied effects of the external tilted magnetic field on the generation of sub-THz/THz high harmonics in the semiconductor superlattice. We showed that the tilted magnetic field can effectively swap the power to THz frequencies. Furthermore, changing the tilt angle of the external magnetic field essentially influences the distribution of spectral power of current oscillations in the semiconductor superlattice and enables us to control them. The obtained results are important for design of new THz generators, based on the superlattices, TEDs and other devices with negative differential conductance.

ACKNOWLEDGMENTS

This work has been supported by the Russian Science Foundation (Grant No. 14-12-00222).

REFERENCES

[1] Bartalini, S., Consolino, L., Cancio, P., De Natale, P., Bartolini, P., Taschin, A., De Pas, M., Beere, H., Ritchie, D., Vitiello, M. S., and Torre, R., "Frequency-comb-assisted terahertz quantum cascade laser spectroscopy," *Phys. Rev. X* **4**, 021006 (2014).

[2] Tekavec, P.F., "High power THz sources for nonlinear imaging," *AIP Conf. Proc.* **253**, 1576 (2014).
[3] Kashiwagi T., "Computed tomography image using sub-terahertz waves generated from a high-tc superconducting intrinsic josephson junction oscillator," *Appl. Phys. Lett.* **104**, 082603 (2014).
[4] Kristinsson, K., Kyriienko, O., and Shelykh, I. A., "Terahertz laser based on dipolaritons," *Phys. Rev. A* **89**, 023836 (2014).
[5] Polyushkin, D. K., Márton, I., Rácz, P., Dombi, P., Hendry, E., and Barnes, W. L., "Mechanisms of THz generation from silver nanoparticle and nanohole arrays illuminated by 100 fs pulses of infrared light," *Phys. Rev. B* **89**, 125426 (2014).
[6] Dekorsy, T., Auer, H., Bakker, H., Roskos, H., and Kurz, H., "THz electromagnetic emission by coherent infrared-active phonons," *Phys. Rev. B* **53**, 4005–4014 (1996).
[7] Chulkov, R., Goryashko, V., Arslanov, D. D., Jongma, R. T., Zande van der, W. J., and Zhaunerchyk, V., "Multimode dynamics in a short-pulse THz free electron laser," *Phys. Rev. ST Accel. Beams* **17**, 050703 (2014).
[8] Gunn, J. B., "Instabilities of current in iiiv semiconductors," *IBM J. Res. Dev.* **8**, 141 (1964).
[9] Koronovskii, A. A., Maksimenko, V. A., Moskalenko, O. I., Hramov, A. E., Alekseev, K. N., and Balanov, A. G., "Transition to microwave generation in semiconductor superlattice," *Physics of wave phenomena* **21**(1), 48–51 (2013).
[10] Selskii, A. O., Koronovskii, A. A., Hramov, A. E., Moskalenko, O. I., Alekseev, K. N., Greenaway, M. T., Wang, F., Fromhold, T. M., Shorokhov, A. V., Khvastunov, N. N., and Balanov, A. G., "Effect of temperature on resonant electron transport through stochastic conduction channels in superlattices," *Phys. Rev. B* **84**, 235311 (2011).
[11] Koronovskii, A. A., Hramov, A. E., Maksimenko, V. A., Moskalenko, O. I., Alekseev, K. N., Greenaway, M. T., Fromhold, T. M., and Balanov, A. G., "Lyapunov stability of charge transport in miniband semiconductor superlattices," *Phys. Rev. B* **88**, 165304 (2013).
[12] Esaki, L. and Tsu, R., "Superlattices and negative differential conductivity in semiconductors," *IBM Journal of Research and Development* **14**(1), 61–65 (1970).
[13] Fromhold, T. M., Patane, A., Bujkiewicz, S., Wilkinson, P. B., Fowler, D., Sherwood, D., Stapleton, S. P., Krokhin, A. A., Eaves, L., Henini, M., Sankeshwar, N. S., and Sheard, F. W., "Chaotic electron diffusion through stochastic webs enhances current flow in superlattices," *Nature* **428**, 726–730 (2004).
[14] Balanov, A. G., Fowler, D., Patane, A., Eaves, L., and Fromhold, T. M., "Bifurcations and chaos in semiconductor superlattices with a tilted magnetic field," *Phys. Rev. E* **77**(2), 026209 (2008).
[15] Greenaway, M. T., Balanov, A. G., Schöll, E., and Fromhold, T. M., "Controlling and enhancing terahertz collective electron dynamics in superlattices by chaos-assisted miniband transport," *Phys. Rev. B* **80**, 205318 (2009).
[16] Hramov, A. E., Koronovskii, A. A., Kurkin, S. A., Makarov, V. V., Gaifullin, M. B., Alekseev, K. N., Alexeeva, N., Greenaway, M. T., Fromhold, T. M., Patane, A., Kusmartsev, F. V., Maksimenko, V. A., Moskalenko, O. I., and Balanov, A. G., "Subterahertz chaos generation by coupling a superlattice to a linear resonator," *Phys.Rev.Lett.* **112**, 116603 (2014).
[17] Wacker, A., "Semiconductor superlattices: a model system for nonlinear transport," *Physics Reports* **357**, 1–111 (2002).